

See discussions, stats, and author profiles for this publication at: <https://www.researchgate.net/publication/263769833>

Side Chain Selection for Designing Highly Efficient Photovoltaic Polymers with 2D-Conjugated Structure

ARTICLE in MACROMOLECULES · JULY 2014

Impact Factor: 5.8 · DOI: 10.1021/ma500829r

CITATIONS

63

READS

108

6 AUTHORS, INCLUDING:



[Shaoqing Zhang](#)

Chinese Academy of Sciences

74 PUBLICATIONS 7,139 CITATIONS

[SEE PROFILE](#)



[Long Ye](#)

North Carolina State University

52 PUBLICATIONS 1,457 CITATIONS

[SEE PROFILE](#)



[Huifeng Yao](#)

Chinese Academy of Sciences

15 PUBLICATIONS 262 CITATIONS

[SEE PROFILE](#)



[Jianhui Hou](#)

Chinese Academy of Sciences

148 PUBLICATIONS 12,322 CITATIONS

[SEE PROFILE](#)

Side Chain Selection for Designing Highly Efficient Photovoltaic Polymers with 2D-Conjugated Structure

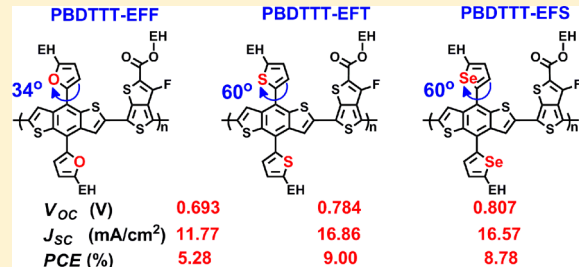
Shaoqing Zhang^{†,‡}, Long Ye,[‡] Wenchao Zhao,[‡] Delong Liu,[‡] Huifeng Yao,[‡] and Jianhui Hou^{*,†,‡}

[†]School of Chemistry and Biology Engineering, University of Science and Technology Beijing, Beijing 100083, China

[‡]State Key Laboratory of Polymer Physics and Chemistry, Beijing National Laboratory for Molecular Sciences, Institute of Chemistry, Chinese Academy of Sciences, Beijing 100190, China

Supporting Information

ABSTRACT: Recently, the benzodithiophene- (BDT-) based polymers with conjugated side groups attracted considerable attention due to their superior properties in polymer solar cells (PSCs), so the investigation of the side chain effects on the photovoltaic properties of this type of polymers is an interesting and important topic for molecular design. Herein, three conjugated polymers based on BDT and thieno[3,4-*b*]thiophene units with furan, thiophene and selenophene as side groups, named as PBDTTT-EFF, PBDTTT-EFT, and PBDTTT-EFS, were synthesized and applied in polymer solar cells. The polymers were characterized in parallel by absorption spectroscopy, thermogravimetric analysis (TGA), density functional theory (DFT), ultraviolet photoemission spectroscopy (UPS), X-ray diffraction (XRD), and photovoltaic measurements. The results show that the dihedral angles between the BDT and conjugated side groups play important roles in affecting the absorption bands, HOMO levels, crystallinities, and aggregation sizes of the polymers. The photovoltaic results indicate that PBDTTT-EFT and PBDTTT-EFS show similar photovoltaic characteristics in device, and PCEs of 9.0% and 8.78% were obtained, respectively. The device of PBDTTT-EFF shows a V_{oc} of 0.69 V and a J_{sc} of 11.77 mA/cm², which are lower than those in the devices based on the other two polymers. Overall, this work suggests that the photovoltaic properties of the BDT-based polymers can be effectively tuned by introducing conjugated side groups with varied steric hindrance.



INTRODUCTION

Conjugated polymers based on benzodithiophene (BDT) units have attracted tremendous interests in the field of polymer solar cells (PSCs). The first application of BDT-based polymers as donor materials in PSCs revealed that the absorption spectra, molecular energy levels, and photovoltaic properties of this type of polymers are highly tunable by copolymerizing BDT units with different conjugated building blocks.¹ In recent years, more and more BDT-based polymers were designed and synthesized, and a few milestone power conversion efficiencies (PCEs) have been recorded by using BDT-based polymers as donor materials in PSCs.^{2–13} On the other hand, the studies of BDT-based polymers also demonstrated several important strategies for molecular design of conjugated polymers for the application in PSCs, and these results have been well summarized and reviewed.^{14,15}

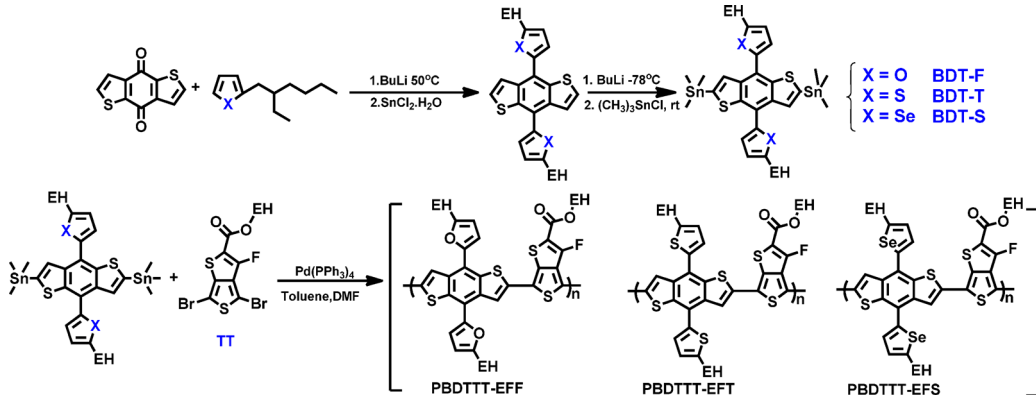
The applications of two-dimensional conjugated (2D) structures in BDT-based polymers have made great progress. For example, our work demonstrated that the BDT-based polymers with 2-alkylthienyl groups exhibited broader absorption bands, higher hole mobilities and better photovoltaic properties compared to their alkoxy substituted analogues; PCE of 7.59%¹⁶ and 8.79%¹⁷ have been realized by utilizing PBDTTT-C-T, one of the representative 2D-BDT-based polymers, as donor material in PSCs with different device

architectures. When varied functional groups were introduced onto the conjugated side groups of the 2D-BDT-based polymers, their molecular energy levels including the highest occupied molecular orbital (HOMO) levels and the lowest unoccupied molecular orbital (LUMO) levels can be effectively tuned without changing their absorption properties, so that the PSC devices with improved open circuit voltages (V_{oc}) and thus enhanced PCEs up to 8.6% have been obtained in the PSC with a conventional device architecture.¹⁸

Varied conjugated side groups have also been used in constructing 2D-BDT-based polymers. For instance, BDT-polymers with *p*-alkylphenyls and *m*-alkoxylphenyl side groups were designed to lower HOMO levels of the polymers and thus to realize higher V_{oc} in PSCs.^{19–21} Very recently, a series of polymers based on thieno[3,4-*c*]pyrrole-4,6-dione (TPD) and 2D-BDT in which furan, thiophene, and selenophene were respectively used as the conjugated side groups were designed to investigate the influence of the conjugated side groups on photovoltaic properties,²² and the reported results indicated that the conjugated side groups play important roles in affecting morphologies of the polymer and phenyl-C₇₁-butyric acid

Received: April 21, 2014

Revised: June 29, 2014

Scheme 1. Synthesis and Molecular Structures of the Monomers and Three Polymers with Varied Conjugated Side Groups

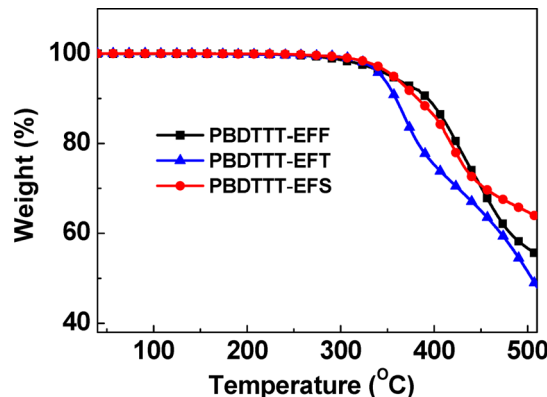
methyl ester (PC_{71}BM) blends. Another recent work reported that the polymer (named as PBDTTT-EFT in Scheme 1) based on of 2-alkylthienyl-substituted BDT and thieno[3,4-*b*]-thiophene show an outstanding PCE of 9.35% in the PSC with inverted structure.²³ Since we did extensive studies on conjugated polymers based on BDT and TT (named as PBDTTTs),^{2,3,14,24,25} we generated the idea of investigating the side chain effects on the photovoltaic properties of PBDTTT-based polymers. Therefore, three polymers named as PBDTTT-EFF, PBDTTT-EFT, and PBDTTT-EFS as shown in Scheme 1 were synthesized and characterized in parallel. The comparison among these three polymers of their properties will provide insights for molecular design of conjugated polymers with varied conjugated side groups. Notably, PBDTTT-EFS is one of the outstanding photovoltaic polymers so far with PCE up to 8.8% and also the best one among selenophene-based photovoltaic polymers. Therefore, these results marked a great advance in applying conjugated side chains in BDT-based polymers.

■ SYNTHESIS OF THE POLYMERS

Herein, as shown in Scheme 1, three BDT monomers with 2-alkylfuryl,^{26,27} 2-alkylthienyl,^{16,23} and 2-alkylselenophenyl²² side groups were copolymerized with the TT units respectively, and three polymers were synthesized and characterized. These three polymers can be easily dissolved into chlorobenzene (CB) and 1, 2-dichlorobenzene (DCB). The number-average molecular weight (M_n) estimated by gel permeation chromatography (GPC) using chloroform as eluent are 5.7 K, 22 and 69 K, with polydispersity index (PDI) 1.85, 2.01, and 2.33. As shown in Figure 1, these three polymers show similar thermal stabilities in the thermogravimetric analysis (TGA), and the decomposition onset points of them are all at ca. 350 °C.

■ THEORETICAL CALCULATIONS OF THE POLYMERS

Density functional theory (DFT) at the B3LYP/6-31G(d, p) level was used to gain insight into the difference of these three BDT units with varied conjugated side groups as well as the corresponding polymers. As shown in Figure 2, for the BDT-F unit, the dihedral angle between the conjugated side group and BDT is 34.1°, which is much smaller than those in BDT-T and BDT-S. The BDT-T and BDT-S units show very similar HOMO levels at ca. -5.12 eV in DFT calculations, while the BDT-F unit has a HOMO level of -4.89 eV. Therefore, it can be speculated that the polymer PBDTTT-EFF may have higher HOMO level than the other two polymers. Furthermore, in

**Figure 1.** Thermogravimetric analysis plots of the three polymers.

order to check the speculation, the DFT method was used to estimate the HOMO and LUMO levels of the dimers of the three polymers. As shown in Figure 2, the HOMO level of the dimer of PBDTTT-EFF is -4.88 eV, which is higher than the other two dimers. In addition, although the HOMO surfaces of these three polymers are well delocalized along their backbones, the conjugation of the side groups in PBDTTT-EFF is more efficient than those of the other two polymers.

■ X-RAY DIFFRACTION ANALYSIS

X-ray diffraction (XRD) measurement has been used to investigate the crystalline properties of conjugated polymers in thin films. Figure 3 shows the XRD patterns of the three conjugated polymers casted from DCB. Obviously, no peak can be found at the region from 2 to 10 degrees, indicating that no ordered laminar packing can be formed in these three polymers. However, as shown in the inset of Figure 3, weak diffraction peaks for $\pi-\pi$ stacking of the polymers can be distinguished. The PBDTTT-EFF film shows a peak at $2\theta = 24.5^\circ$, corresponding to a $\pi-\pi$ stacking *d*-spacing of 3.63 Å; both the PBDTTT-EFT and PBDTTT-EFS films show diffraction peaks at ca. 22.5°, which are corresponding to *d*-spacing of 3.94 Å. According to the XRD results, PBDTTT-EFF shows more compact $\pi-\pi$ stacking than the other two polymers, which should be ascribed to the smaller dihedral angle in BDT-F than those in BDT-T and BDT-S.

■ ABSORPTION SPECTRA

Parts a and b of Figure 4 show the UV-visible absorption spectra of the three polymers in dilute solution and in solid

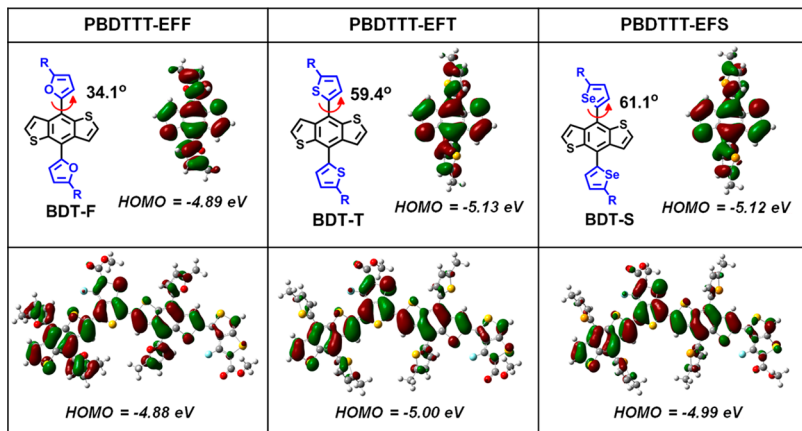


Figure 2. Theoretical calculations of the BDT units and dimers of the three polymers by density functional theory (DFT) at the B3LYP/6-31G(d, p) level.

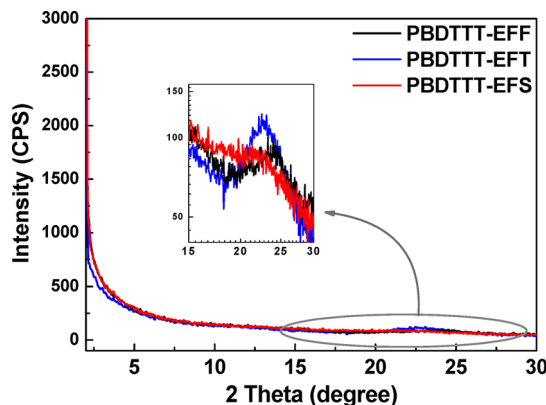


Figure 3. X-ray diffraction patterns of three types of polymer films casted from DCB onto Si substrates.

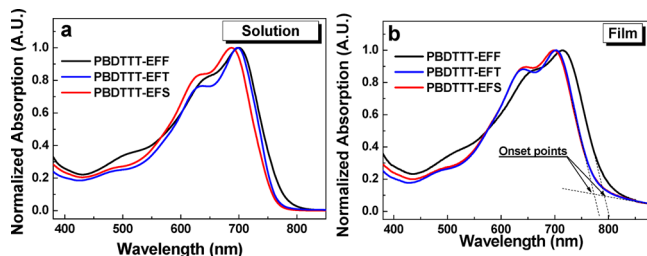


Figure 4. Absorption spectra of three polymers in dilute chloroform (a) and in solid film (b).

film, and the corresponding results are collected in Table 1. All of the three polymers show similar profiles both in solution and solid state. Compare to the spectra in solution, the absorption

Table 1. Optical Properties and Molecular Energy Levels of the Polymers

polymer	optical properties of the films					
	λ_{max} (nm)	λ_{edge} (nm)	E_g^{opt} (eV)	ϵ (10^4 cm^{-1})	HOMO (eV)	LUMO (eV)
PBDTTT-EFF	720	800	1.55	7.82	-5.19	-3.64
PBDTTT-EFT	700	785	1.58	8.02	-5.24	-3.66
PBDTTT-EFS	699	785	1.58	7.78	-5.29	-3.71

peaks in solid films of all these three polymers are red-shifted. The films of PBDTTT-EFT and PBDTTT-EFS exhibit very similar optical properties in the whole absorption range; i.e., both two absorption spectra show peaks at ca. 700 nm and onsets at ca. 785 nm, corresponding to optical band gaps (E_g^{opt}) of 1.58 eV. In comparison with PBDTTT-EFT and PBDTTT-EFS, the absorption spectrum of the PBDTTT-EFF film shows a red-shifted peak at 720 nm and a smaller E_g^{opt} of 1.55 eV. As mentioned above, smaller dihedral angle is obtained in BDT-F than in BDT-T and BDT-S, so the side groups in PBDTTT-EFF have more efficient conjugation with the backbone than those in the other two polymers, which might be the main reason for the red-shifted absorption spectrum of PBDTTT-EFF. In addition, these three polymers have similar absorption coefficients in thin films, which are 7.82×10^4 , 8.02×10^4 , and 7.78×10^4 per centimeter for PBDTTT-EFF, PBDTTT-EFT, and PBDTTT-EFS, respectively.

MOLECULAR ENERGY LEVEL MEASUREMENTS

Ultraviolet photoelectron spectroscopy (UPS) was employed as an effective tool to evaluate the energy levels of photovoltaic polymers.²⁸ Parts a and b of Figure 5 show onset and high

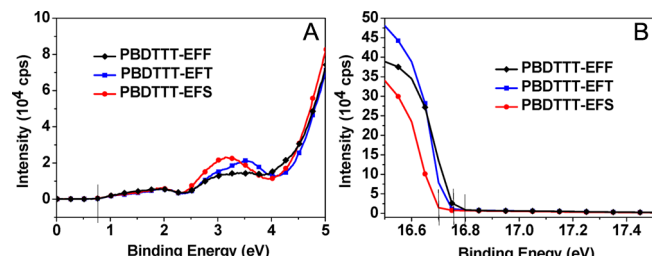


Figure 5. UPS spectra of (a) the onset and (b) the secondary edge region of PBDTTT-EFF, PBDTTT-EFT, and PBDTTT-EFS.

binding energy cutoff region of thin films of the three polymers, respectively. As known, the HOMO levels could be determined using the incident photon energy, $h\nu = 21.22 \text{ eV}$, E_{cutoff} and the E_{onset} . The HOMO levels of PBDTTT-EFF, PBDTTT-EFT, and PBDTTT-EFS are indicated in Table 1. Thus, the LUMO levels were calculated using the HOMO levels and the optical gaps (E_g^{opt}). The UPS results reveals that the polymer PBDTTT-EFF shows the highest HOMO level among these three polymers, and PBDTTT-EFT and PBDTTT-EFS show

similar HOMO levels. These results are coincident with the values obtained by the theoretical calculations.

PHOTOVOLTAIC PROPERTIES

PSC devices were fabricated to evaluate and compare the photovoltaic properties of these three polymers. Herein, a commonly used device structure of ITO/PEDOT:PSS/polymer:PC₇₁BM/Ca/Al was employed and the devices of the three polymers were fabricated in parallel. The active layers of the devices were prepared by using DCB as processing solvent. The polymer/PC₇₁BM (D/A) ratios used in all of the devices are 1:1.5 (w/w) and small amount of 1,8-diiodooctane (DIO) is used to optimize their photovoltaic performance; these conditions are similar as those of other analogue polymers based on BDT and TT units such as PBDTTT-C-T,¹⁶ PBDTTT-E,²⁹ and PTB7.³⁰ The concentrations of DIO including 1%, 3%, 5% were respectively tested for three polymers, and the corresponding results were listed in the Supporting information, Table S1 and Figure S1. Moreover, the error bars for photovoltaic parameters were also depicted in Figure S2. Clearly, 3% is the optimal volume amount of DIO for three photovoltaic polymers.

Figure 6a depicts the current density–voltage (*J*–*V*) curves of the PSC devices based on the three polymers, which were

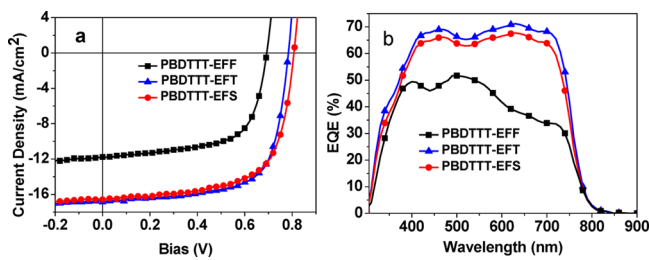


Figure 6. (a) Current density–voltage (*J*–*V*) curves of the PSCs based on polymer/PC₇₁BM (1:1.5, w/w) with 3% DIO (v/v) as additive under the illumination of AM 1.5G (100 mW/cm²). (b) External quantum efficiency (EQE) curve of the corresponding devices.

fabricated under the optimal conditions. The corresponding photovoltaic data obtained from the *J*–*V* curves are listed in Table 2. As shown, the device of PBDTTT-EFF shows a *V*_{oc} of

Table 2. Photovoltaic Properties of the PSCs Based on the Blend of Polymer/PC₇₁BM (1:1.5, w/w) with 3% DIO (v/v) as Additive under the Illumination of AM 1.5G, 100 mW/cm²

polymer	<i>V</i> _{oc} [V]	<i>J</i> _{sc} [mA/cm ²]	FF [%]	PCE [%]	thickness [nm]
PBDTTT-EFF	0.693	11.77	64.81	5.28	90
PBDTTT-EFT	0.784	16.86	68.16	9.00	100
PBDTTT-EFS	0.807	16.57	65.64	8.78	98

0.69 V, which is the lowest one in these three types of PSCs. Compared to the device of PBDTTT-EFF, the devices based on PBDTTT-EFT and PBDTTT-EFS show higher *V*_{oc} values, which are 0.78 and 0.80 V, respectively. The devices of PBDTTT-EFT and PBDTTT-EFS show similar short circuit current densities of 16.86 mA/cm² and 16.57 mA/cm² respectively, which are higher than that of the device of PBDTTT-EFF. All these three polymers show similar fill

factors (FF) at around 0.65, which are among the good values for the BDT-based polymers.^{2–13} The overall efficiencies of the devices based on PBDTTT-EFT and PBDTTT-EFS are 9.0% and 8.78%, respectively, which are much higher than that of the device of PBDTTT-EFF. The external quantum efficiency curves of the devices are demonstrated in Figure 6b. It shows that the EQE curves of these three types of devices have similar response range and similar profiles, which can cover the whole visible range. The PBDTTT-EFF device shows lower EQE values than the other two devices, which is coincident with the *J*–*V* measurements, i.e. the integral *J*_{sc} of the PBDTTT-EFF device is much lower than those of the other two devices.

MORPHOLOGY STUDY

The surface morphology properties of the polymer:PC₇₁BM blend films were tested by using atomic force microscopy (AFM). The topography and phase images of the polymer:PC₇₁BM blend films prepared under the same conditions are shown in Figure 7. The blend films of PBDTTT-EFT:PC₇₁BM and PBDTTT-EFS:PC₇₁BM show very similar morphological properties. For example, the mean square surface roughness (*R*_q) of the films of PBDTTT-EFT:PC₇₁BM and PBDTTT-EFS:PC₇₁BM (see Figure 7, parts c and e) are 2.08 and 1.59 nm respectively; the phase images of these two films are similar and the aggregation sizes observed in Figure 7, parts d and f, are around tens of nanometer. However, the blend film of PBDTTT-EFF:PC₇₁BM shows distinct morphological features compared to the other two films. As shown in parts a and b of Figure 7, the aggregation size reaches hundreds nanometer scale, which is the biggest one in these three films; the *R*_q of the film is 5.19 nm, which is 2–3 folds of those of the other two films. Obviously, the aggregation size in the PBDTTT-EFF:PC₇₁BM blend is too big to get efficient EQE, because the exciton diffusion length in organic semiconductors is 10–20 nm only³¹ and thus big size aggregation in the blend will cause strong geminate recombination. The results show that the polymer with furan side groups will induce strong aggregation in the blend, while the polymers with thiophene and selenophene show better compatibility with PC₇₁BM.

Furthermore, transmission electron microscope (TEM) was applied to confirm the phenomena observed in the AFM measurements. TEM images of the three blend films processed with the optimum conditions are shown in Figure 8a–c. Apparently, larger size aggregations can be clearly observed in the TEM image of the PBDTTT-EFF:PC₇₁BM blend (see Figure 8a); however the aggregation size seems smaller than that observed in the topography and phase images in the AFM measurements. This results indicate that the blend of PBDTTT-EFF:PC₇₁BM has smaller aggregations in the bulk than on the top surface. From parts b and c of Figure 8, it can be found that the blend of PBDTTT-EFT:PC₇₁BM shows a uniform phase separation in the bulk, while slight phase separation can be observed in the blend of PBDTTT-EFS:PC₇₁BM. Overall, the TEM measurements are coincident with the observations from the AFM measurements, and the phenomena observed in this work are quite similar to the reported results of the polymers based on 2D-BDT and TPD.²² Therefore, we can conclude that the polymers based on the BDT units with furan side groups have the tendency to form large size aggregations in the polymer:PCBM blend, which is unfavorable to device performance, while the polymers based on the BDT units with thiophene or selenophene side groups

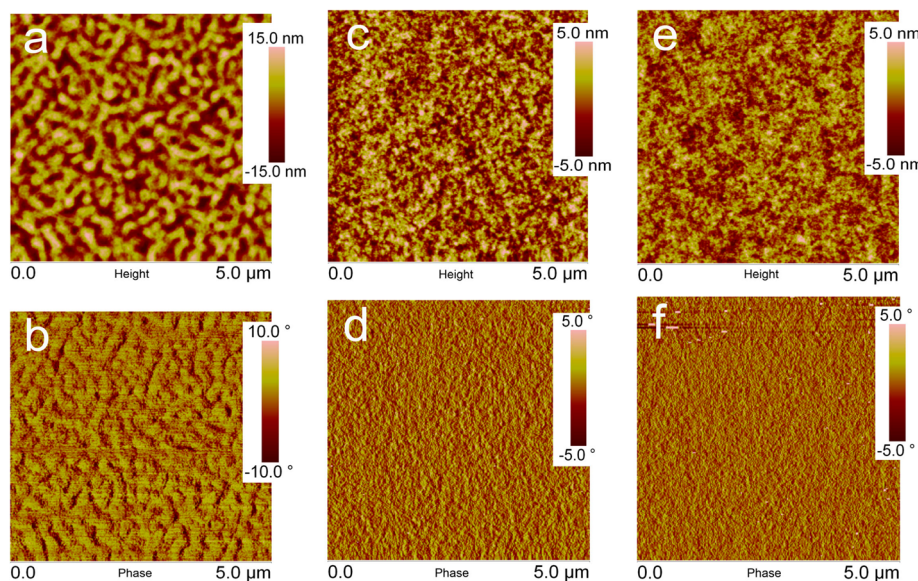


Figure 7. Tapping-mode AFM images: topography image and phase image of the blend films of PBDTTT-EFF:PC₇₁BM (a, b), PBDTTT-EFT:PC₇₁BM (c, d), and PBDTTT-EFS:PC₇₁BM (e, f) processed with DCB and 3% (v/v) DIO.

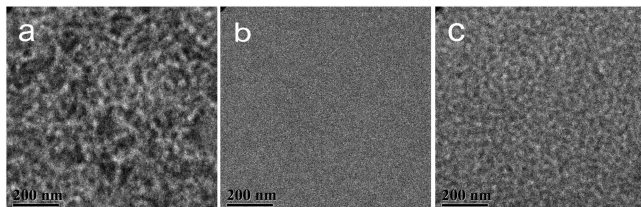


Figure 8. TEM images of the blend films of PBDTTT-EFF:PC₇₁BM (a), PBDTTT-EFT:PC₇₁BM (b), and PBDTTT-EFS:PC₇₁BM (c) processed with DCB and 3% (v/v) DIO.

have better compatibility with PCBM, which is good for forming favorable phase separation in the blend.

OVERALL CONSIDERATION OF THE THREE TYPES OF CONJUGATED SIDE GROUPS

When we put all of the results together, the following picture emerges. For the polymer with furan units as the side groups, smaller dihedral angle and thus more planar conjugated structure will be formed in the BDT part of the polymer; when thiophene or selenophene were used as the side groups, the dihedral angles between the side groups and BDT will be increased. The comparison among the $\pi-\pi$ stacking distance of these three polymers reveals that a smaller dihedral angle of the conjugated side group is helpful to form more compact $\pi-\pi$ stacking. However, the enhanced interchain $\pi-\pi$ stacking effect will cause problems in realizing nanoscale phase separation in the polymer:PCBM blend. This part of results indicate that in the polymers based on the 2D-BDT units, the polymers based on the thiophene or selenophene side groups keep a good balance to get the conjugation of the side groups and interchain interaction in aggregation state. That is to say, the dihedral angle between the side group and BDT plays important role in affecting morphological properties of the polymer.

Moreover, we speculate that the dihedral angle also plays an important role in affecting molecular energy levels of the polymers. As illustrated in Table 3, we used DFT method to carry out the molecular simulation to investigate the effect of the dihedral angle. Herein, the redundant function was used to

Table 3. HOMO Levels of Three BDT Units with Different Dihedral Angles in their Side Groups by Theoretical Calculations

		θ	HOMO (eV)
BDT-F		34.1°	-4.89
		60°	-5.11
BDT-T		34°	-4.94
		59.4°	-5.13
BDT-S		34°	-4.93
		61.1°	-5.12

freeze the dihedral angel of BDT-F to 60 degree, which is the same as that in optimized structure of BDT-T and BDT-S; the dihedral angles of BDT-T and BDT-S were also frozen to 34 degree, which is the same as that in BDT-F. The HOMO levels of these three BDT units with optimized structures and redundant functions are collected in Table 3. For BDT-F unit, when the dihedral angle increases from 34° to 60°, the HOMO level of BDT-F reduces from -4.89 to -5.11 eV; for BDT-T and BDT-S units, when the dihedral angles reduce from ~60° to 34°, the HOMO level elevate from ca. -5.12 eV to ca. -4.9 eV. The results reveal that since furan, thiophene and selenophen are all π -electron rich units, their electron donating effect will be reduced when the dihedral angles are increased. As a result, the polymer PBDTTT-EFF shows a higher HOMO level than the other two polymers.

CONCLUSION

In this work, two new polymers (PBDTTT-EFF and PBDTTT-EFS) were synthesized and characterized with a reported polymer (PBDTTT-EFT). In these three polymers, different conjugated side groups including 2-alkylfuryl, 2-alkylthienyl, and 2-alkylselenophenyl were used to get the 2D conjugated structure. The computational results reveal that the furan side groups show weaker steric hindrance and thus smaller dihedral angle to the backbones than the other two types of conjugated side groups, so that the polymer PBDTTT-EFF show a $\pi-\pi$ stacking distance of 3.63 Å, which is smaller than those in PBDTTT-EFT and PBDTTT-EFS. The photovoltaic results indicate that PBDTTT-EFT and PBDTTT-EFS show similar photovoltaic characteristics in device, and PCEs of 9.0% and 8.78% were obtained, respectively. The device of PBDTTT-EFF shows a V_{oc} of 0.69 V and a J_{sc} of 11.77 mA/cm², which are lower than those in the devices based on the other two polymers. The morphological results reveal that oversized aggregations are formed in the PBDTTT-EFF:PC₇₁BM blend, which can be ascribed to the strong interchain $\pi-\pi$ stacking effect of the polymer due to the low steric hindrance of the conjugated side groups. Overall, this work suggests that not only molecular energy levels but also morphologies of the BDT-based polymers can be effectively tuned by introducing conjugated side groups with varied steric hindrance.

EXPERIMENTAL SECTION

Materials Synthesis. Reagents. The three BDT monomers, BDT-F,^{26,27} BDT-T,^{16,23} and BDT-Se²² were synthesized by the reported methods. The TT monomer, 2-(2-ethylhexyl)-4,6-dibromo-3-fluorothieno[3,4-*b*]thiophene-2-carboxylate was purchased from Solarmer Materials Inc. Pd(PPh₃)₄ was purchased from Frontier Scientific Inc. [6,6]-Phenyl-C₇₁-butyric acid methyl ester (PC₇₁BM) was purchased from Orgatec Materials, Inc. All of the commercial available compounds and reagents were used without any further treatment.

Synthesis of PBDTTT-EFF. BDT-F (0.5 mmol) and the TT monomer (0.5 mmol) were dissolved into a mixture of toluene (10 mL) and dimethylformamide (DMF, 2 mL). The solution was flushed with argon for 5 min and Pd(PPh₃)₄ (25 mg) was successively added into the flask. Then, the mixture was flushed with argon for another 20 min and stirred at 110 °C for 16 h under the argon atmosphere. After cooling down to room temperature, the polymer was precipitated by pouring into methanol (100 mL) and then collected by filtration. The resultant polymer was extracted successively with acetone (4 h) and hexane (6 h) by using Soxhlet extraction apparatus. The remaining solid was extracted with 200 mL of chloroform. After evaporation under reduced pressure, the concentrated solution was precipitated in 100 mL of methanol and the polymer was collected by filtration.

PBDTTT-EFT and PBDTTT-EFS were synthesized by the same procedure used in PBDTTT-EFF.

PBDTTT-EFF: Anal. Calcd for C₄₉H₅₇FO₄S₄: C, 68.65; H, 6.70. Found: C, 68.90; H, 6.79.

PBDTTT-EFT: Anal. Calcd for C₄₉H₅₇FO₂S₆: C, 66.17; H, 6.46. Found: C, 66.39; H, 6.42.

PBDTTT-EFS: Anal. Calcd for C₄₉H₅₇FO₂S₄Se₂: C, 59.86; H, 5.84. Found: C, 60.07; H, 5.96.

Instruments and Measurements. UV-visible absorption spectroscopy measurements were carried out using a Hitachi U-3100 UV-vis spectrophotometer. TGA measurement was performed on TGA-2050 from TA Instruments, Inc. Atom force microscopy (AFM) was performed on a Nanoscope V (Vecco) AFM by tapping mode. Molecular weight and polydispersity (PDI) of the polymers were estimated by gel permeation chromatography (GPC) method by using monodispersed polystyrene as standard and chloroform as eluent. A set of samples were analyzed on the Thermo Scientific ESCALab

250Xi using UPS. The gas discharge lamp was used for UPS, with helium gas admitted and the He I (21.22 eV) emission line employed. The helium pressure in the analysis chamber during analysis was about 2 × 10⁻⁸ mbar. The data were acquired with -10 V bias.

The current density–voltage (*J*–*V*) characteristics were recorded with an Agilent B2912A Precision Source/Measure unit. The power conversion efficiencies of the polymer solar cells were measured under 1 sun, AM 1.5G (air mass 1.5 global) (100 mW/cm²), using a XES-70S1 (SAN-EI ELECTRIC CO., Ltd.) solar simulator (AAA grade, 70 mm × 70 mm photobeam size). Two × 2 cm silicon reference cell (KG3 filter) was purchased from Enli Technology Co., Ltd. The external quantum efficiency (EQE) was measured by a Solar Cell Spectral Response Measurement System QE-R3011 (Enli Technology Co., Ltd.). The light intensity at each wavelength was calibrated with a standard single-crystal Si photovoltaic cell.

Fabrication of Polymer Solar Cells. Polymer solar cell devices with the structure of ITO/PEDOT:PSS/Polymers:PC₇₁BM/Ca(20 nm)/Al(80 nm) were fabricated under conditions as follows: patterned indium tin oxide (ITO)-coated glass with a sheet resistance of 10–15 ohm/square was cleaned by a surfactant scrub and then washed by deionized water, acetone and isopropanol, successively. After UV–ozone cleaning for 15 min, a 35 nm thick poly(3,4-ethylenedioxythiophene):poly(styrenesulfonate) (PEDOT:PSS) (Bayer Baytron 4083) anode buffer layer was spin-cast onto the ITO substrate and then dried in an oven at 150 °C for 15 min. The active layer, with a thickness in the range of 80–110 nm, was then deposited on top of the PEDOT:PSS layer by spin-coating from a *o*-dichlorobenzene solution of certain concentration (15 mg/mL), with 1,8-diiodooctane (3% by volume) as additive. Then, small amount of methanol was spin-coated on the blend film at 4000 rpm for 30 s to remove the residual additives.³² Finally, 20 nm Ca and 80 nm Al layer were successively deposited under high vacuum (ca. 2 × 10⁻⁴ Pa) onto the active layer. The overlapping area between the cathode and anode defined a pixel size of 4 mm². Except for the deposition of the PEDOT:PSS layers, all the fabrication processes were carried out inside a nitrogen glovebox containing less than 10 ppm oxygen and moisture.

ASSOCIATED CONTENT

Supporting Information

¹H NMR spectra of the monomers (BDT-F, BDT-T, BDT-S, TT) and the polymers, IR spectra of the polymers (PBDTTT-EFF, PBDTTT-EFT, PBDTTT-EFS), and photovoltaic data of the devices made by varied fabrication processes. The information is available free of charge via the Internet at <http://pubs.acs.org>.

AUTHOR INFORMATION

Corresponding Author

*(J.H.) E-mail: hjhzlz@iccas.ac.cn.

Notes

The authors declare no competing financial interest.

ACKNOWLEDGMENTS

The authors would like to acknowledge the financial support from Ministry of Science and Technology of China, International S&T Cooperation Program of China (2011DFG63460), the Science and Technology Commission of Beijing (Z131100006013002), the Chinese Academy of Science (Nos. XDB12030200, KJZD-EW-J01), NSFC (Nos. 21325419, 51373181, 51261160496).

REFERENCES

- (1) Hou, J.; Park, M. H.; Zhang, S.; Yao, Y.; Chen, L. M.; Li, J. H.; Yang, Y. *Macromolecules* **2008**, *41*, 6012.

- (2) Chen, H. Y.; Hou, J.; Zhang, S.; Liang, Y.; Yang, G.; Yu, L.; Wu, Y.; Li, G. *Nat. Photonics* **2009**, *3*, 649.
- (3) Hou, J.; Chen, H. Y.; Zhang, S.; Chen, R. I.; Yang, Y.; Wu, Y.; Li, G. *J. Am. Chem. Soc.* **2009**, *131*, 15586.
- (4) Liang, Y.; Yu, L. *Acc. Chem. Res.* **2010**, *43*, 1227.
- (5) Piliego, C.; Holcombe, T. W.; Douglas, J. D.; Woo, C. H.; Beaujuge, P. M.; Frechet, J. M. J. *J. Am. Chem. Soc.* **2010**, *132*, 7595.
- (6) Price, S. C.; Stuart, A. C.; Yang, L.; Zhou, H.; You, W. *J. Am. Chem. Soc.* **2011**, *133*, 4625.
- (7) Zhou, H.; Yang, L.; Stuart, A. C.; Price, S. C.; Liu, S.; You, W. *Angew. Chem., Int. Ed.* **2011**, *50*, 2995.
- (8) Wang, M.; Hu, X.; Liu, P.; Li, W.; Gong, X.; Huang, F.; Cao, Y. *J. Am. Chem. Soc.* **2011**, *133*, 9638.
- (9) Chen, H. C.; Chen, Y. H.; Liu, C. C.; Chien, Y. C.; Chou, S. W.; Chou, P. T. *Chem. Mater.* **2012**, *24*, 4766.
- (10) Li, K.; Li, Z.; Feng, K.; Xu, X.; Wang, L.; Peng, Q. *J. Am. Chem. Soc.* **2013**, *135*, 13549.
- (11) Liu, P.; Zhang, K.; Liu, F.; Jin, Y.; Liu, S.; Russell, T. P.; Yip, H. L.; Huang, F.; Cao, Y. *Chem. Mater.* **2014**, *26*, 3009.
- (12) Cui, C.; Wong, W. Y.; Li, Y. *Energy Environ. Sci.* **2014**, *7*, 2276.
- (13) Ye, L.; Zhang, S.; Zhao, W.; Yao, H.; Hou, J. *Chem. Mater.* **2014**, *26*, 3603.
- (14) Huo, L.; Hou, J. *Polym. Chem.* **2011**, *2*, 2453.
- (15) Ye, L.; Zhang, S.; Huo, L.; Zhang, M.; Hou, J. *Acc. Chem. Res.* **2014**, *47*, 1595.
- (16) Huo, L.; Zhang, S.; Guo, X.; Xu, F.; Li, Y.; Hou, J. *Angew. Chem., Int. Ed.* **2011**, *50*, 9697.
- (17) Li, X.; Choy, W. C. H.; Huo, L.; Xie, F.; Sha, W. E. I.; Ding, B.; Guo, X.; Li, Y.; Hou, J.; You, J.; Yang, Y. *Adv. Mater.* **2012**, *24*, 3036.
- (18) Zhang, M.; Guo, X.; Zhang, S.; Hou, J. *Adv. Mater.* **2014**, *26*, 1118.
- (19) Dou, L.; Gao, J.; Richard, E.; You, J.; Chen, C. C.; Cha, K. C.; He, Y.; Li, G.; Yang, Y. *J. Am. Chem. Soc.* **2012**, *134*, 10071.
- (20) Zhang, M.; Guo, X.; Ma, W.; Zhang, S.; Huo, L.; Ade, H.; Hou, J. *Adv. Mater.* **2014**, *26*, 2089.
- (21) Zhang, M.; Gu, Y.; Guo, X.; Liu, F.; Zhang, S.; Huo, L.; Russell, T. P.; Hou, J. *Adv. Mater.* **2013**, *25*, 4944.
- (22) Warnan, J.; El Labban, A.; Cabanetos, C.; Hoke, E. T.; Shukla, P. K.; Risko, C.; Brédas, J.-L.; McGehee, M. D.; Beaujuge, P. M. *Chem. Mater.* **2014**, *26*, 2299.
- (23) Liao, S. H.; Jhuo, H. J.; Cheng, Y. S.; Chen, S. A. *Adv. Mater.* **2013**, *25*, 4766.
- (24) Huang, Y.; Huo, L.; Zhang, S.; Guo, X.; Han, C. C.; Li, Y.; Hou, J. *Chem. Commun.* **2011**, *47*, 8904.
- (25) Huang, Y.; Guo, X.; Liu, F.; Huo, L.; Chen, Y.; Russell, T. P.; Han, C. C.; Li, Y.; Hou, J. *Adv. Mater.* **2012**, *24*, 3383.
- (26) Jiang, J. M.; Lin, H. K.; Lin, Y. C.; Chen, H. C.; Lan, S. C.; Chang, C. K.; Wei, K. H. *Macromolecules* **2014**, *47*, 70.
- (27) Wang, Y.; Yang, F.; Liu, Y.; Peng, R.; Chen, S.; Ge, Z. *Macromolecules* **2013**, *46*, 1368.
- (28) Gong, X.; Tong, M.; Brunetti, F. G.; Seo, J.; Sun, Y.; Moses, D.; Wudl, F.; Heeger, A. J. *Adv. Mater.* **2011**, *23*, 2272.
- (29) Liang, Y.; Wu, Y.; Feng, D.; Tsai, S. T.; Son, H. J.; Li, G.; Yu, L. *J. Am. Chem. Soc.* **2009**, *131*, 56.
- (30) Liang, Y.; Xu, Z.; Xia, J.; Tsai, S. T.; Wu, Y.; Li, G.; Ray, C.; Yu, L. *Adv. Mater.* **2010**, *22*, E135.
- (31) Clarke, T. M.; Durrant, J. R. *Chem. Rev.* **2010**, *110*, 6736.
- (32) Ye, L.; Jing, Y.; Guo, X.; Sun, H.; Zhang, S.; Zhang, M.; Huo, L.; Hou, J. *J. Phys. Chem. C* **2013**, *117*, 14920.